Optically-active 1-D MoS$_2$ nano-belts

Akshay A. Murthy[#],[†] Yuan Li[#],[†],[‡] Edgar Palacios, [‖] Qianqian Li,[†],[‡] Shiqiang Hao,[†] Jennifer G. DiStefano, [†],[§] Chris Wolverton,[†] Koray Aydin,[‖] Xinqi Chen,[†],[‡] Vinayak P. Dravid [*],[†],[‡],[§]

[#]A. M. and Y. L. Contributed equally to this work

[†]Department of Materials Science and Engineering, [‡]Northwestern University Atomic and Nanoscale Characterization Experimental (NU*ANCE*) Center, [§]International Institute for Nanotechnology (IIN), and [‖]Department of Electrical Engineering and Computer Science, Northwestern University, Evanston, Illinois 60208, USA

*Corresponding author

Vinayak P. Dravid: v-dravid@northwestern.edu

S1. Experimental details

S1.1 Synthesis of MoS$_2$ nanobelts

MoS$_2$ nanobelts were synthesized via a modified atmospheric pressure CVD growth process. 5 mg of MoO$_3$ powder (Sigma-Aldrich) was evenly spread in an alumina boat and two face-down 300 nm SiO$_2$/Si or Si substrates were suspended above the boat. This assembly was placed within a 1-inch diameter quartz tube and at the center of a one zone furnace. Another alumina boat containing 130 mg sulfur powder (Sigma-Aldrich) was placed upstream outside of the furnace. Following a 15 min purge of the tube with ultra-high purity argon gas, the temperature at the center of the furnace was heated to a growth temperature of 700°C over a period of 40 min and held at that temperature for 3 min. When the temperature of the center region reached 600°C, a magnet was used to bring the alumina boat containing sulfur to a region inside the furnace where the temperature was ~150°C, thereby initiating the CVD reaction. The growth was conducted at atmospheric pressure while flowing 13 sccm of ultra-high purity argon gas. The furnace was subsequently allowed to cool naturally.

S1.2 Sample characterization

Raman and PL spectra were obtained using a Horiba LabRAM HR Evolution Confocal Raman system under laser illumination with a wavelength of 532 nm and a power of 0.5mW. X-ray Photoelectron spectroscopy (XPS) was conducted using a Thermo Scientific ESCALAB 250Xi system with charge referenced to adventitious C1s, C-C peak at 284.8eV. Hitachi SU8030 SEM and JEOL JEM-2100 FasTEM were used to examine the structure and morphology of the nanobelts. Reflection mapping was conducted using a broadband Halogen light source and a Nikon inverted microscope coupled into a 303-mm-focal-length spectrometer containing an

Andor Newton electron multiplication charge-coupled device (EM-CCD) detector. The x-y piezo stage was computer controlled and set to 500nm step size over a 2.7um x 2.7um region. The spectrometer is equipped with a physical slit which can close below 100um, allowing us to capture data from a region below 1um using a 100x objective with 0.9 NA. In the final measurements, data was taken from an area equivalent to ~479nm x 479nm region using both pixel binning and the physical slit before the spectrometer entrance.

S1.3 Simulations

2D-electromagnetic wave numerical calculations were performed using the finite-difference time-domain simulation software package Lumerical™ to simulate scattering from a standalone MoS_2 nano-belt. The simulation region was 500 x 500 x 2000 nm in XYZ which is large enough to eliminate potential simulation errors from evanescent fields which can prevent convergence in the simulation. The boundary conditions were set to perfectly matched layers (PML) perpendicular to and parallel to the propagation direction. The source used was a total-field scattered-field (TFSF) to separate the total field and scattered field. The scattered field was captured by a group of power monitors surrounding the source while the absorption in the nano-belt was calculated from a group of power monitors surrounding the nano-belt. A mesh overwrite region was to 1nm x 1nm over the MoS_2 nano-belt to ensure simulation accuracy. Refractive indices were taken from literature for MoS_2 from Beal [1] and Si from Palik [2] while the SiO_2 index was set to a constant 1.45.

S1.4 Sample Transfer

Poly (methyl methacrylate) (PMMA) (950 PMMA A3, Micro Chem) was first spin coat over the nanobelt sample before 2M KOH solution was used to etch the underlying SiO_2. The released film was then placed onto another substrate and the PMMA was dissolved in acetone and isopropanol.

S1.5 Device Fabrication

The device fabrication was conducted using a standard photolithography process using a maskless laser aligner. Briefly, photoresist (S1813) was spin-coated on the substrate with a spin rate of 4000 rpm for 30 s. The substrate was soft-baked at 110°C for 1 min. The pre-designed contact mask (electronic) was aligned to the device target region. UV light exposure was then conducted for 26 ms with a defocus of -1. The substrate was then developed in MF-319 for 45 s and further cleaned with oxygen plasma at 100 W for 3 min. Subsequently, a 5-nm Cr film and 50-nm Au film were thermally evaporated onto the substrate to serve as the contact. The sample was then lifted off in hot acetone and finally annealed at 250 °C for 2 h (in Ar environment) before optoelectronic characterization. Electrical measurements were carried out in a probe-station using an Agilent 4155C Semiconductor Parameter Analyzer.

S1.6 Density Functional Theory (DFT) Calculations

Density functional theory (DFT) electronic structure calculations were performed on the MoS_2 3R crystal to gain insight into the material's band gap. While the effect of dimensional confinement on the band structure of the 2H and 1T MoS_2 polytypes have been thoroughly examined, we deemed it necessary to understand whether our system (3R phase) evolved with

varying size at the measured dimensions of the MoS_2 nano-belts. Since, we detected no changes to the electronic structure at these magnitudes, the representative bulk values are provided here. The total energies and relaxed geometries were calculated by DFT within the generalized gradient approximation (GGA) of Perdew-Burke-Ernzerhof the exchange correlation functional with Projector Augmented Wave potentials [3]. We use periodic boundary conditions and a plane wave basis set as implemented in the Vienna ab initio simulation package [4]. The spin-orbital coupling effects are included for the band structure calculations. The total energies were numerically converged to approximately 3 meV/cation using a basis set energy cutoff of 500 eV and dense k-meshes corresponding to 4000 k-points per reciprocal atom in the Brillouin zone.
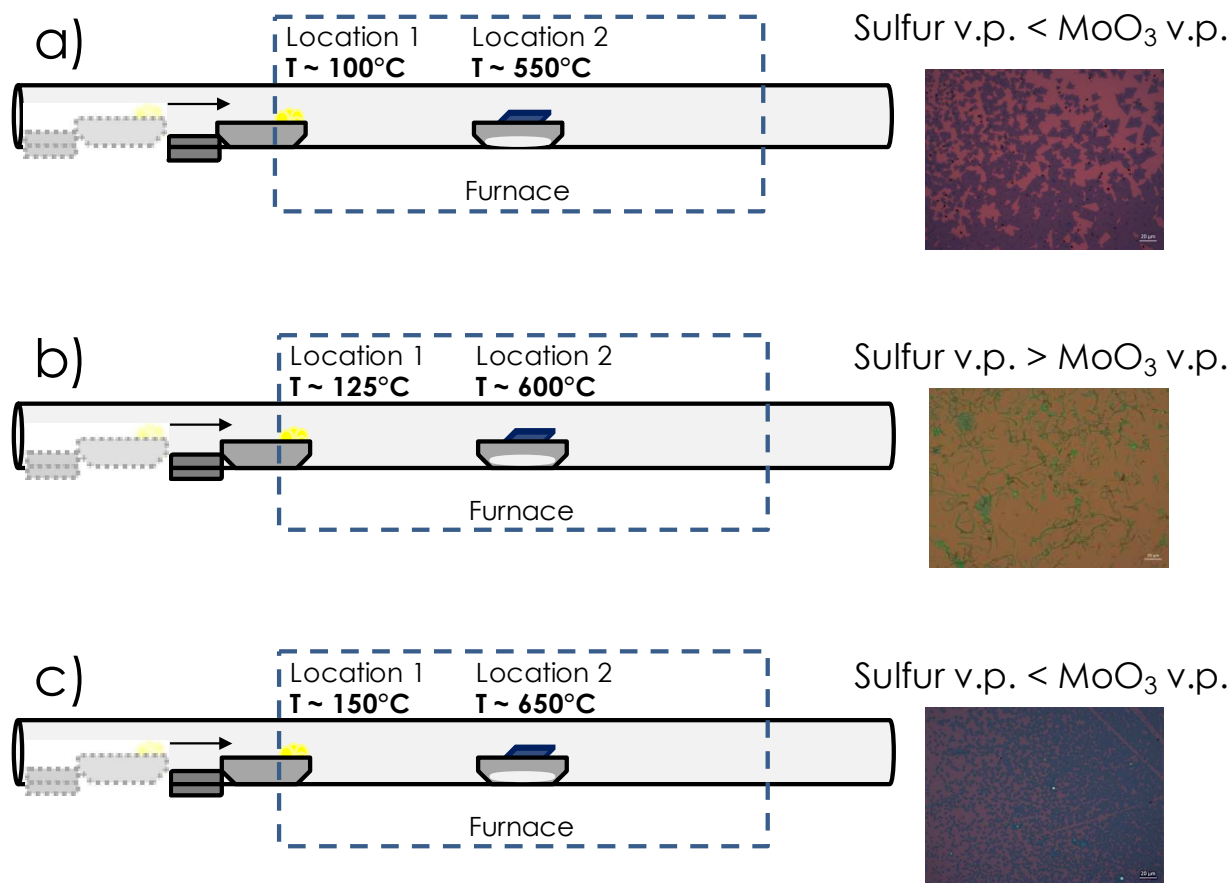
Figure S1. Schematic indicating MoS₂ growth setup and synthesized products depending on different conditions used. (a) In the first case, the sulfur was introduced into location 1 within the furnace (~100°C) when the center of the furnace was at 550°C and monolayer flakes were synthesized. (b) In the second case, the sulfur was introduced into location 1 within the furnace (~125°C) when the center of the furnace was at 600°C and nanobelts were synthesized. We postulate that this is due to the initially sulfur-rich atmosphere. (c) In the final case, the sulfur was introduced into location 1 within the furnace (~150°C) when the center of the furnace was at 650°C and once again, monolayer flakes were synthesized. Note: v.p. stands for vapor pressure.
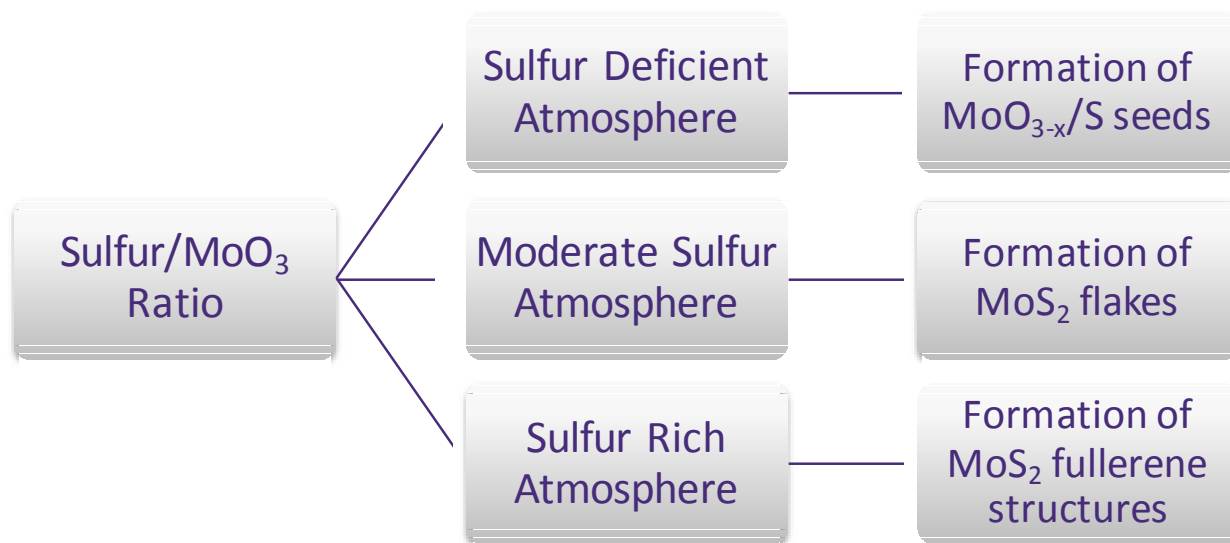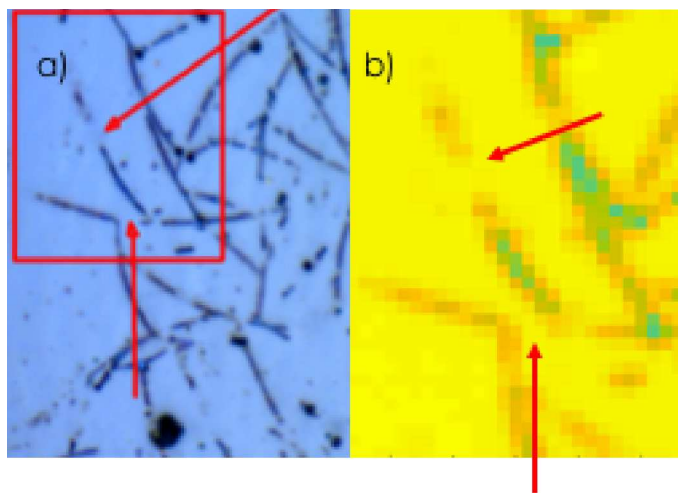
**Figure S2. Roadmap detailing possible products from MoO₃ reaction with sulfur**
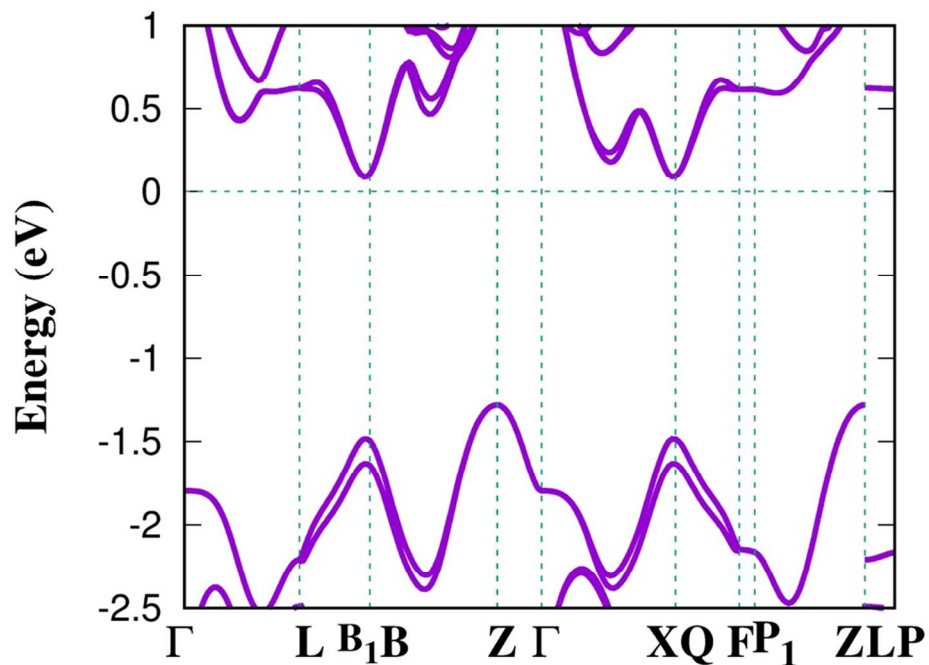
Figure S3. DFT calculations of band structure for 3R MoS$_2$ nano-belts. Band gap is 1.36 eV and indirect. Calculations performed with spin orbit coupling included.

Figure S4. Reflectance Map. (a) CCD image of the region of interest and (b) Reflectance map of region of interest for 725 nm wavelength, corresponding to the scattering peak predicted by FDTD calculations
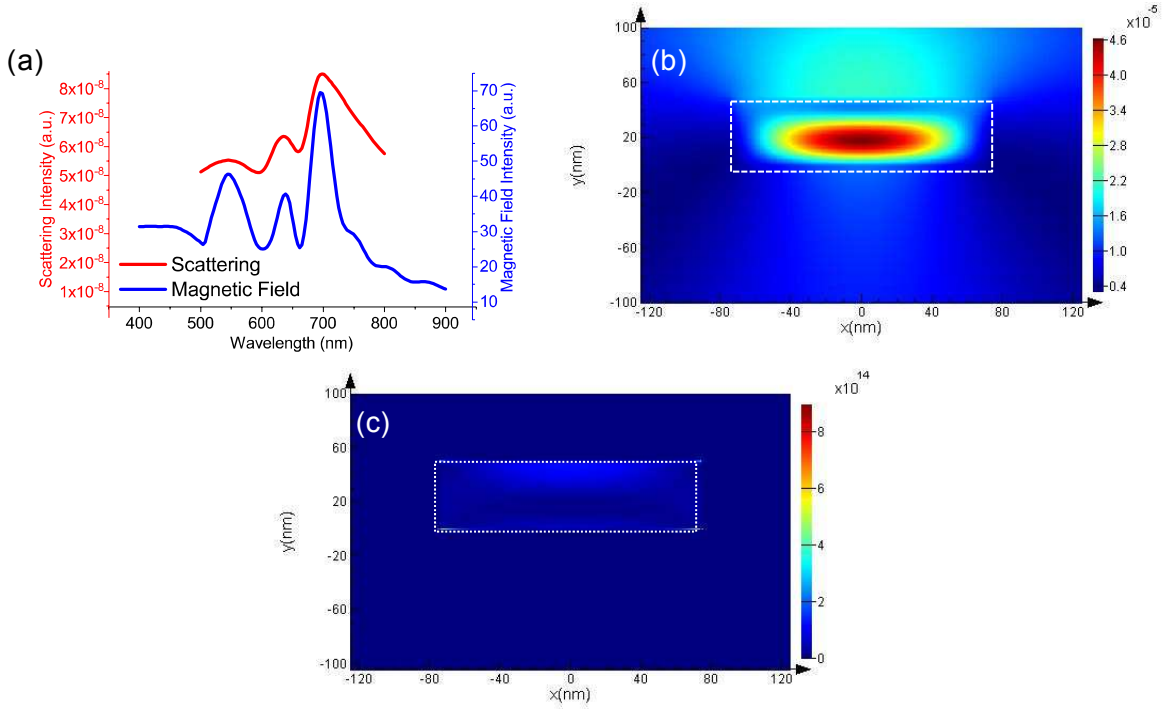
Figure S5. Magnetic modes in MoS₂ nano-belt. (a) FDTD simulations detailed in S1.3 were used to calculate the magnetic field (H) intensity within the MoS₂ nano-belt as a function of illumination wavelength. As apparent, magnetic field maxima within the nano-belt are seen at 545 nm, 635 nm and 700 nm, which correspond well with peaks seen in the scattering spectrum. (b) $|H|^2$ field map for nano-belt at λ=545nm, (c) Power absorption map at λ=545nm. It is apparent that an appreciable amount of power is absorbed by the nano-belt, which can induce photogenerated carriers. The white dotted lines indicate the nano-belt.
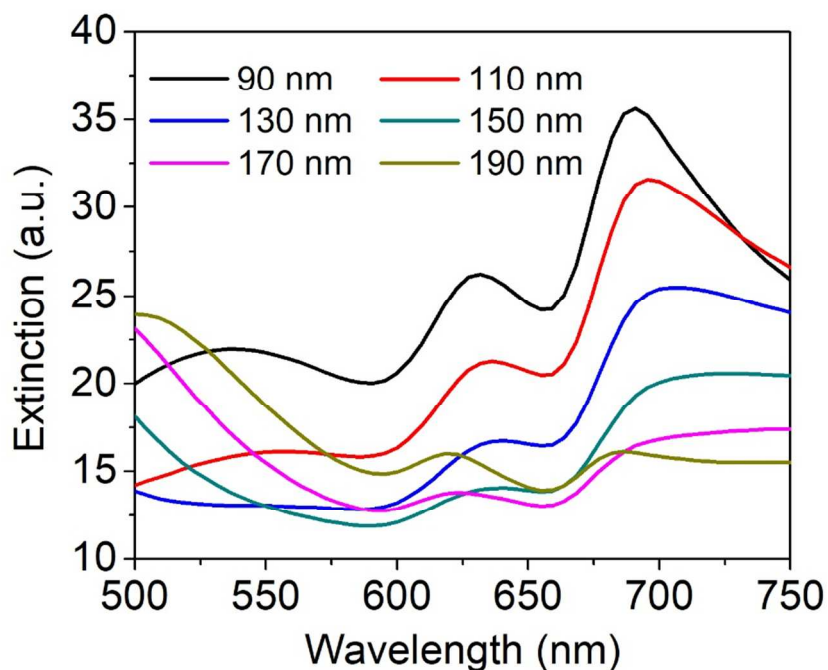
Figure S6. FDTD simulations for nanobelts with different widths. The extinction spectra for MoS_2 nanobelts with widths varying from 90nm – 190nm are shown using FDTD calculations detailed in S1.3. In the case where d=90nm, one magnetic field resonance mode is apparent at 550 nm. As can be seen, this mode red-shifts and becomes broader with increasing width. For d=190nm, this mode is no longer apparent in this range of wavelengths, however, the next mode (~500nm) is now visible.

References:

1. Beal, A.; Hughes, H., Kramers-Kronig analysis of the reflectivity spectra of 2H-MoS2, 2H-MoSe2 and 2H-MoTe2. *Journal of Physics C: Solid State Physics* **1979,** *12* (5), 881-890.

2. Edwards, D., " Silicon (Si)," in Handbook of Optical Constants of Solids. *Palik ed. Academic, Orlando, Fla* **1985**. 547-569.

3. Perdew, J. P.; Burke, K.; Ernzerhof, M. Phys. Rev. Lett. 1996, 77, No. 3865.

4. Kresse, G.; Furthmüller, J. Phys. Rev. B 1996, 54, No. 11169.